INFLUENCE OF ANNEALING UNDERLOAD ON MAGNETO-OPTICAL PROPERTIES OF IRON-BASED NANOCRYSTALLINE RIBBONS

© 2025 A. M. Kharlamova[a, *], P. Y. Kozhevnikova[a], T. P. Kaminskaya[a], G. V. Kurlyandskaya[b], E. E. Shalygina[a]

[a]*Faculty of Physics, Moscow State University, Moscow, Russia*

[b]*Institute of Natural Sciences and Mathematics, Ural Federal University, Ekaterinburg, Russia*

**e-mail: anna-h-m@mail.ru*

Received November 15, 2024

Revised December 14, 2024

Accepted December 30, 2024

Abstract. The results of the influence of load annealing on the magneto-optical properties of soft magnetic nanocrystalline $Fe_{68.5}Cr_5Si_{13.5}B_9Nb_3Cu_1$ ribbons obtained by rapid quenching from the melt and then annealed at a temperature of 520 °C for 2 h without load and using a specific load of 150 MPa are presented. The near-surface magnetic hysteresis loops and simultaneous visualization of the changes of magnetic domain structure were measured using a magneto-optical Kerr magnetometer. The obtained experimental data that annealing underload leads to the formation of induced magnetic anisotropy and affects the magnetic field behavior of the samples.

Keywords: *annealing under load, magnetic anisotropy, magnetic domain structure, magneto-optical Kerr effect, soft magnetic materials*

DOI: 10.31857/S03676765250417e3

INTRODUCTION

In the last three decades, nanostructured magnetically soft ferromagnetic iron-based alloys have attracted great attention both in terms of fundamental research and for technological applications because of their unusual structural, electrical, magnetic, optical properties and corrosion resistance [1,2]. In particular, the structure and magnetic properties of the so-called feinmet (FM) class of alloys (Fe-based alloy− Si− Nb-B-Cu) have been investigated. This material, obtained as ribbons by rapid quenching from the melt, or thin magnetic films, acquires excellent magnetically soft properties, which allows its widespread application in the electrical and radio industries, electronic engineering and instrumentation [3-5]. Comparatively recently, new alloys have been created by alloying with chromium or molybdenum and modifying the classical composition (FeCuNbSiB) with feinmet, resulting in higher crystallization temperature and improved corrosion resistance of the alloys [1, 4-6]. Amorphous ribbons are usually annealed at temperatures above the primary crystallization temperature, which is approximately 510 °C, to obtain optimum structure and properties. It was found that the lowest value of the coercivity of $Fe_{73.5}Si_{13.5}Nb_3Cu_{(1)\ B9}$alloy is observed at an annealing temperature of 520° °C. The deterioration of magnetically soft properties with increasing annealing temperature from 520 to 580° C is explained by the decrease of silicon concentration in FeSi

nanocrystals, which leads to an increase in the magnetocrystalline anisotropy constant from 8.4 to 11.2 $kJ \cdot m^{-3}$[6]. In addition, it has been shown that the induced magnetic anisotropy is a special tool for tuning the magnetic responses, allowing to control the magnitude of dynamic and static magnetic permeability by means of stress annealing [2, 7]. Until now, the question of searching for the most effective composition of tapes remains relevant. One of the methods for investigating the features of induced anisotropy is the magneto-optical Kerr effect [8]. In the framework of this work, the influence of stress annealing on the magnetic anisotropy features and magneto-optical properties of $Fe_{68.5}Cr_5Si_{(13.5)\ B9}Nb_3Cu_1$composition tapes, including their dependence on the geometrical features of the samples, was investigated for the first time.

STUDIED SAMPLES

The amorphous $Fe_{68.5}Cr_5Si_{(13.5)\ B9}Nb_3Cu_1$ribbons studied in this work were were obtained by rapid quenching from the melt on a rotating copper drum. Two series of samples were studied: strips annealed at 520° C for 2 h without load (relaxation annealing, FM-AN) and strips annealed at 520 ºC for 2 h using a specific load of 150 MPa (FM-SA). This annealing temperature was chosen as the optimum temperature to obtain samples with the most pronounced magnetically soft properties. During annealing, the samples were fixed on both sides by mechanical clamps and placed in a zone of high temperature uniformity in a vertical furnace. Weights of a given value were suspended from the lower clamp. The specific load was calculated based on the specimen cross-section and weight of the load. In each series (FM-AN and FM-SA), two tapes of different widths (c) of 0.88 mm (FM1 and FM4) and 0.60 mm (FM2 and

FM3) were fabricated in order to evaluate the influence of edge effects for specimens with smaller widths. The thickness of each tape (*b*) was 20.0 ± 0.2 μm.

The studied samples were mechanically cut off from the initial tapes and had a rectangular shape. The length of samples (*a*) did not exceed 4 mm, which was due to the technical data of the experimental setup for the study of magneto-optical properties. In addition, this size is optimal for the operation of detectors of weak magnetic fields based on the giant magnetic impedance effect [7].

The geometric parameters of the studied tapes were estimated from photographs obtained on an optical microscope and measured using an electronic caliper. The masses of the samples required for the subsequent magnetization determination were determined using high-precision electronic scales immediately before the magnetic characteristics measurements.

EXPERIMENTAL METHODS

The structure of the studied $Fe_{68.5}Cr_{(5)}Si_{(13.5)\ B9}Nb_3Cu_1$ribbons was investigated by X-ray diffraction using $CuK_{(\alpha)\ (}$wavelength λ= 1.5418 Å).

The surface morphology of the samples was investigated by optical and atomic force microscopy (AFM) using a scanning probe microscope SMENA-A, "Solver" platform (NT-MDT, Zelenograd) in semi-contact mode at room temperature. We used standard silicon cantilevers MFM 01 with resonance frequencies from 47 to 90 kHz, needle tip radius of 40 nm, force constant 1-5 $N \cdot m^{-1}$. Samples were scanned in areas of sizes 4× 4, 12× 12 and 30× 30 μm^2. The obtained AFM images were processed using mathematical operations and filters of the program "Nova" provided by the manufacturers of the standard AFM package.

The measurement of the near-surface hysteresis loops and simultaneous visualization of the magnetic domain structure (MD) features in the process of sample remagnetization (changes in the magnetization component (*M*) under the action of the applied magnetic field were recorded) were performed using a magneto-optical Kerr-magnetometer at room temperature from the free side of the tapes, i.e., the side of the tapes that was not in contact with the drum surface during their production. The Kerr-magnetometer used is based on a Carl Zeiss polarizing microscope (Manufacturer: Evico magnetics GmbH, Germany). DS was observed using the meridional Kerr effect (MEK) proportional to the magnetization component parallel to the plane of light incidence. The external magnetic field (*H*) was applied in the plane of the tapes in two directions: $\theta = 0°$ and $90°$, where θ is the angle between the tape axis and the direction of propagation of *H*. The principle of contrast image acquisition using the above microscope is as follows. First, the original image of the specimen is registered. The presence of different contrast colors corresponds to the fact that the magnetization vectors *M* in these regions are directed in different directions. Image processing requires contrast enhancement. In this connection, a topographic contrast image, i.e., a background image of the sample, is registered in a magnetic field exceeding the saturation field. Computer processing of these data allows us to obtain a difference image that contains only the contrast corresponding to the magnetic domains.

RESULTS AND DISCUSSION

Figure 1 shows the results of X-ray phase analysis of $Fe_{68.5}Cr_{(5)}Si_{(13.5)\,B9}Nb_3Cu_1$of AN and SA tapes. These studies showed that the samples have a nanocrystalline

structure with a crystallite size calculated by the Scherrer method of about 15 ± 3 nm. The additional peaks after annealing resulted from a slight oxidation of the surface, which does not affect the main magnetic characteristics. The background consists of much broader peaks, the contribution to which comes predominantly from the amorphous matrix (matrix composition− Fe(Nb)-B). In addition to the main peaks from Fe-Si nanocrystals, the regions with superstructural ordering, the regions of the Fe_3Si phase, make a noticeable contribution to the diffractogram.

The most characteristic surface images and surface profiles of the investigated samples annealed without load and under load, obtained by AFM, are presented in Fig. 2.

Analysis of the obtained data showed that for samples annealed without load (FM-AN, Fig. *2a* and *2b*), the average surface roughness of the samples (R_a) is of the order of 20.0± 0.1 nm, and the deviation of the surface profile from the average value ΔZ, of the order of 100 nm. For the stress annealed samples (FM-SA, Fig. *2c* and *2d*), $R_a \approx 10$ nm, and $\Delta Z \approx 20.0 \pm 0.1$. That is, $R_a$and ΔZ for FM-SA samples, are smaller than those for FM-AN. Moreover, the values of ΔZ can differ by an order of magnitude. Thus, the stress annealing procedure leads to a decrease in surface roughness. This result has never been discussed in studies on the magnetodynamic properties of ribbon-shaped samples. The change of the dynamic magnetic permeability was previously always interpreted in terms of the appearance of transverse magnetic anisotropy with a small dispersion of the light magnetization axes [2, 7]. In this case, the roughness reduction can significantly reduce the contribution of surface anisotropy and increase

the degree of homogeneity of the ferromagnetic sample properties and provide an additional increase in magnetic permeability.

Typical near-surface magnetic hysteresis loops of the studied tapes measured at angles θ equal to 0° and 90° , annealed unloaded and loaded are shown in Figs. 3 и 4.

It can be seen that the magnetic field behavior of the tapes depends on θ: at θ= 0° the hysteresis loops have an almost rectangular shape (black curves), while at θ=90° a more complex, inclined shape of the hysteresis loop is observed (red curves). In addition, for FM1 (Fig. *3a*) and FM3 (Fig. *4b*) tapes, the remagnetization of the tape samples at θ= 90° proceeds in two steps.

The data of Figures 3 and 4 also show that for the same width ribbons, annealing under load affects the magnetic field behavior of samples: the shape of magnetic hysteresis loops for samples annealed under load (Figures 3b and *4b*) differs from the shape of hysteresis loops of samples annealed without load (Figures *3a* and *4a*), respectively. The main reason for the appearance of induced magnetic anisotropy after annealing under load is considered to be the residual deformation of the lattice of nanocrystals [2,9,10].

In particular, it was found that annealing under load affects the values of coercive force ($H_{C)}$: at c = 0.88 mm, a decrease in $H_{(C)}$values by a factor of about 2 is observed, while at c = 0.60 mm, an increase in $H_C$values by a factor of about 2. It is known that stress annealing leads to the formation of transverse magnetic anisotropy of the "difficult plane" type. The addition of Cr leads to an increase in H_C, also the volume fraction of nanocrystallites formed during annealing decreases [11].

It is found that changing the geometry of the strip affects the values of H_C. It can be seen from Figs. *4b* and *3b*, it can be seen that as the width of the strip annealed under load decreases, the values of $H_C$increase by about 2.7 times. At the same time, for the specimen annealed without load Figs. *4a* and *3a*, a decrease in $H_C$values by a factor of about 1.3 is observed.

Comparison of the near-surface $H_C$values with the previously obtained bulk $H_C$values showed that the near-surface values are an order of magnitude larger than the bulk values. This fact can be explained by the presence of microstructural and chemical heterogeneities in the near-surface layers of the samples at a depth of up to 100 nm, which is characteristic of materials prepared by the described method of quenching from the melt [12].

Images of the magnetic domain structure were also obtained. Typical DS speciation of the studied tapes is shown in the insets of Figs. 3 и 4. It can be seen that for samples annealed without load (Fig. 3), the general appearance of the magnetic domain structure agrees well with the ideas about magnetic domains of magnetically soft material [8]: broad domains with magnetization oriented in the plane and in opposite directions in neighboring domains are observed. When remagnetizing in the direction of the short side of the tape, the picture becomes somewhat more complicated, since the direction along the tape axis is the direction of light magnetization. At$\theta = 90^o$, the remagnetization is carried out along the axis of difficult magnetization, but the previously mentioned features of surface roughness lead to increased inhomogeneity of the magnetization process. The decrease of magnetic contrast in this configuration

confirms the position about the contribution of rotation processes and is also confirmed by the shape of magnetic hysteresis loops.

Evaluating the role of geometry, we can conclude that for FM1 and FM2 samples annealed without loading (Figs. *3a* and *4a*), broad domains with 180 ° domain walls are observed, which is typical for soft ferromagnetic materials with uniaxial magnetic anisotropy [7].

For the samples annealed under load (Figs. 3b and 4b), the dependence of the magnetic domain structure features on the angle θ is observed, which is to be expected for a material with induced magnetic anisotropy. After stress annealing, an interesting situation arises where the shape anisotropy (light magnetization axis - direction along the long side of the ribbon) and the induced magnetic anisotropy (light magnetization axis - direction along the short side of the ribbon) are in competition. Experimental data show that the remagnetization of samples in the geometryθ = 0°is mainly due to the displacement of domain boundaries, and atθ = 90°mainly by rotation of the magnetization vector *M*. A typical well-defined zigzag domain structure is observed for the stress annealed samples [13,14]. In addition, for the FM3 sample annealed under load (Fig. *4b*), both band and zigzag domain structures are observed simultaneously. The observed domain structures are consistent with the characteristics of the hysteresis loops discussed above.

CONCLUSION

As a result of the conducted study of $Fe_{68.5}Cr_5Si_{(13.5)\ B9}Nb_3Cu_1$nanocrystalline ribbons in the states after relaxation annealing and after stress annealing, quantitative

characteristics of surface morphology, structure features, magnetic and magneto-optical properties have been determined. It was found that the studied samples have a nanocrystalline structure with crystallite size of about 15 ± 3 nm. It was found that loading during annealing leads to a significant decrease in the surface roughness of the ribbons, which may be a factor affecting the increase in the dynamic magnetic permeability of materials of this type. It is found that the reduction of the ribbon width from 0.88 to 0.60 mm affects the $H_C$value: for samples annealed without load, it decreases about 1.3 times, for samples annealed under load, it increases about 2.7 times. It is shown that loading during annealing leads to the formation of transverse magnetic anisotropy, apparently, as a consequence of residual deformation of the lattice of nanocrystals. Annealing under load and the direction of external field application affect the magnetic field behavior of samples and magneto-optical properties: samples annealed without load have broad domains with domain walls of 180° , samples annealed under load have simultaneously banded and zigzag magnetic domain structure, and a chaotic distribution of magnetization depending on θ is observed. The experimental results obtained can be used for the fabrication of alloys with predetermined properties, including materials for inductors and detectors of weak magnetic fields.

REFERENCES

1. *McHenry M., Willard M.A., Laughlin D.E.* // Progr. Mater. Sci. 1999. V 44. P. 291.
2. *Kurlyandskaya G.V., Lukshina V.A., Larrañaga A. et al.* // J. Alloys Compounds. 2013. V. 566. P. 31.
3. *Ershov N.V., Llukshina V.A., Fedorov V.I. et al.* // Phys. Solid State. 2013. V. 55. No. 3. P. 508.

4. *Serikov V.V., Kleinerman N.M., Volkova E.G. et al. //* Phys. Metal. Metallogr. 2006. V. 102. P. 268.

5. *Moulin J., Mazaleyrat F., Mendez A., Dufour-Gergam E.* // J. Magn. Magn. Mater. 2010. V. 322. P. 1275.

6. *Ershov N.V., Chernenkov Y.P., Fedorov V.I. et al. //* Phys. Solid State. 2021. V. 63. No. 7. P. 978.

7. *Vazquez M., Kurlyandskaya G.V., Garcia-Beneytez J.M. et al. //* IEEE Trans. Magn. 1999. V. 35. No. 5. P. 3358.

8. *Hofmann B., Kronmuller H. //* J. Magn. Magn. Mater. 1996. V.152. No. 91. P. 91.

9. *Ohnuma M., Hono K., Yanai T. et al.* // Appl. Phys. Lett. 2003. V. 83. No. 14. P. 2859.

10. *Mironov V.L.* Fundamentals of Scanning Probe Microscopy. Nizhny Novgorod: IFM RAS, 2004. 114 c.

11. *Ershov N.V., Fedorov V.I., Chernenkov Y.P. et al.*// Phys. Solid State. 2017. V. 59. No. 9. P. 1748.

12. *Shalygina E.E., Molokanov V.V., Komarova M.A.* // JETP. 2002. V. 95. P. 511.

13. *Kurlyandskaya G.V., Lezama L., Pasynkova A.A. et al.* // Materials. 2022. V. 15. P. 4160.

14. *Hubert A., Schäfer R.* Magnetic Domains. Berlin: Springer, 1998. P. 686.

FIGURE CAPTIONS

Figure 1. X-ray spectra observed for the studied samples annealed without loading (blue curve - FM-AN) and under loading (red curve - FM-SA).

Figure 2. AFM surface image (*a*, *c*) and surface profile (*b*, *d*) obtained for FM1 tape (*a*, *b*) annealed without load and FM4 (*c*, *d*) annealed under load.

Figure 3. Near-surface hysteresis loops measured in the magnetic field applied in the plane of the ribbons annealed without load (FM1) and under load (FM4) with width $c = 0.88$ mm using an MO Kerr magnetometer.

Figure 4. Near-surface hysteresis loops measured in the magnetic field applied in the plane of tapes annealed without load (FM2) and under load (FM3) with width $c = 0.60$ mm using an MO Kerr magnetometer.

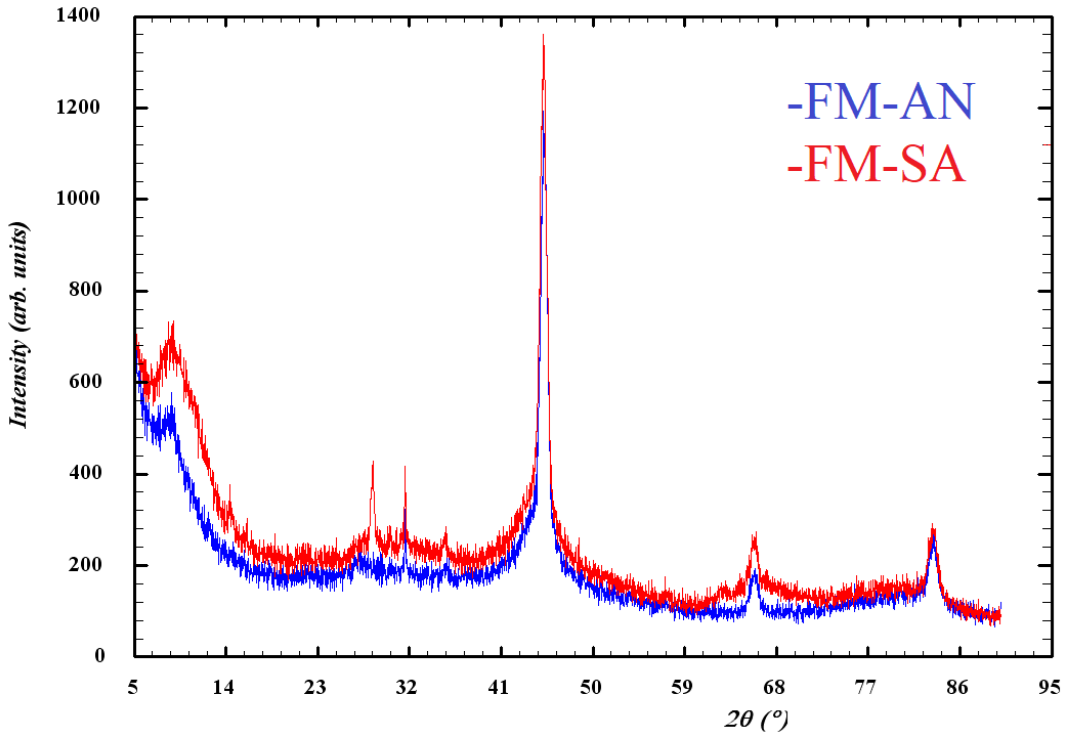

Fig. 1.

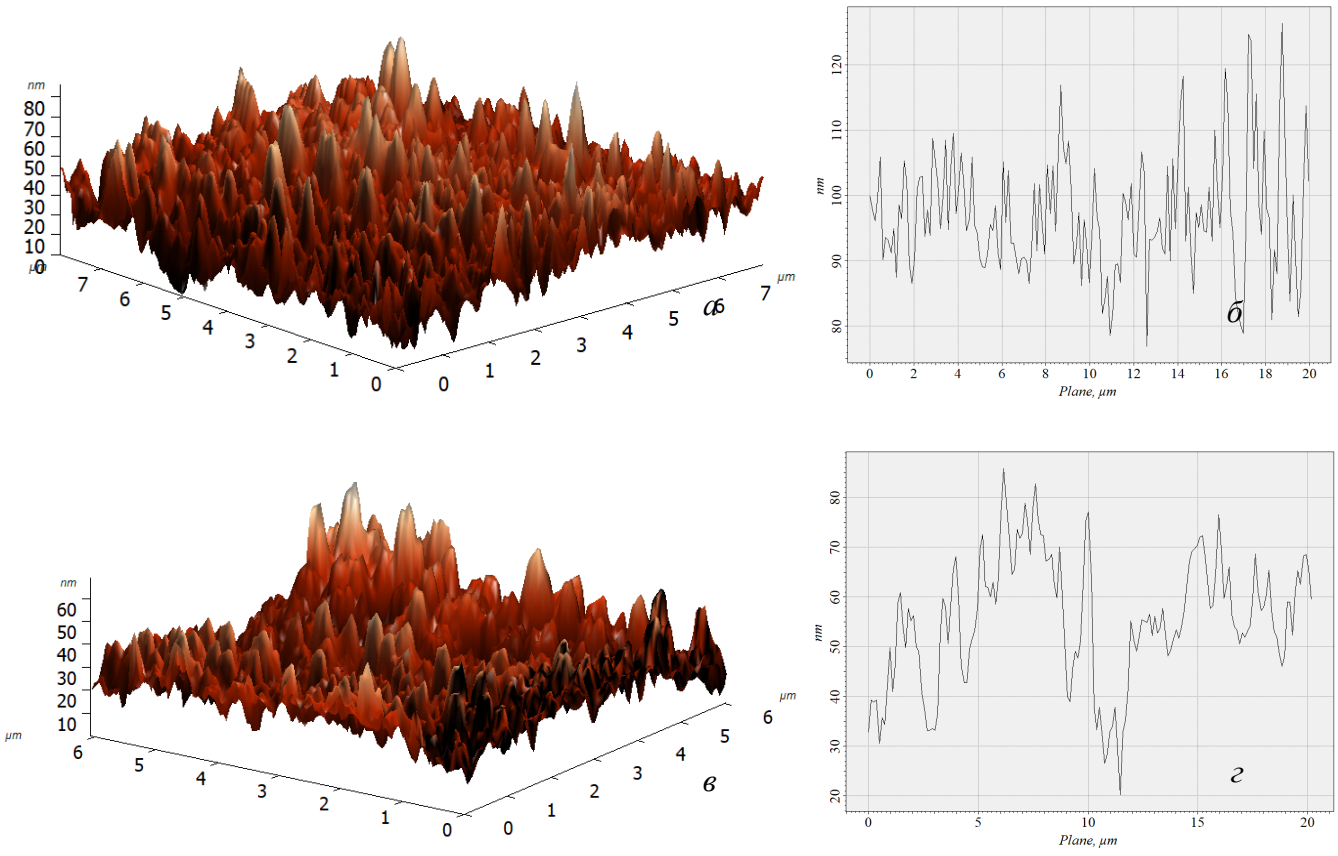

Fig. 2.

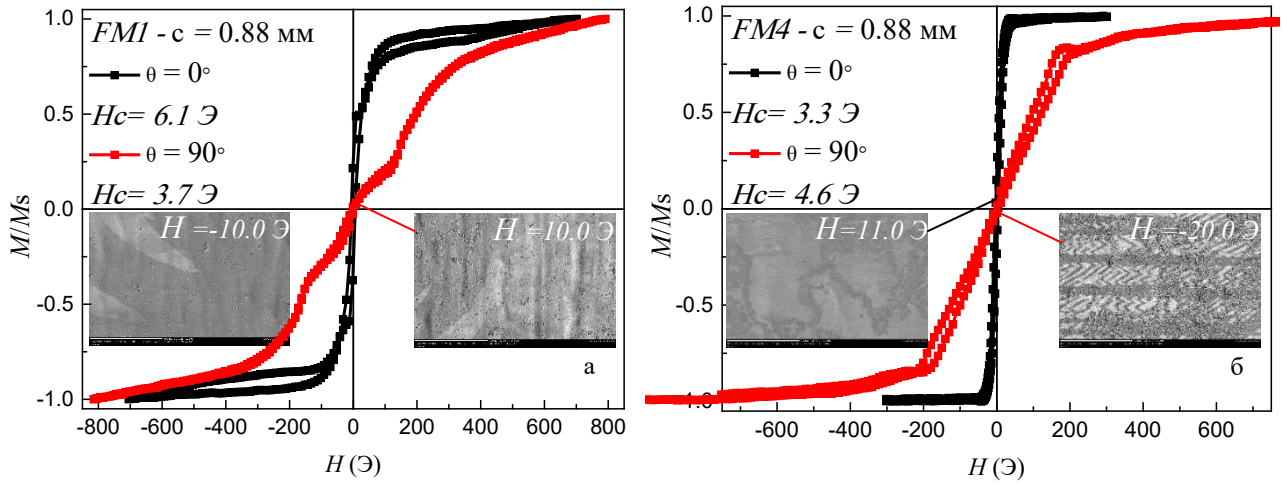
FM1 - c = 0.88 мм
θ = 0°
Hc= 6.1 Э
θ = 90°
Hc= 3.7 Э
H =-10.0 Э
H =10.0 Э
а
FM4 - c = 0.88 мм
θ = 0°
Hc= 3.3 Э
θ = 90°
Hc= 4.6 Э
H=11.0 Э
H =-20.0 Э
б
M/Ms
H (Э)

Fig. 3.

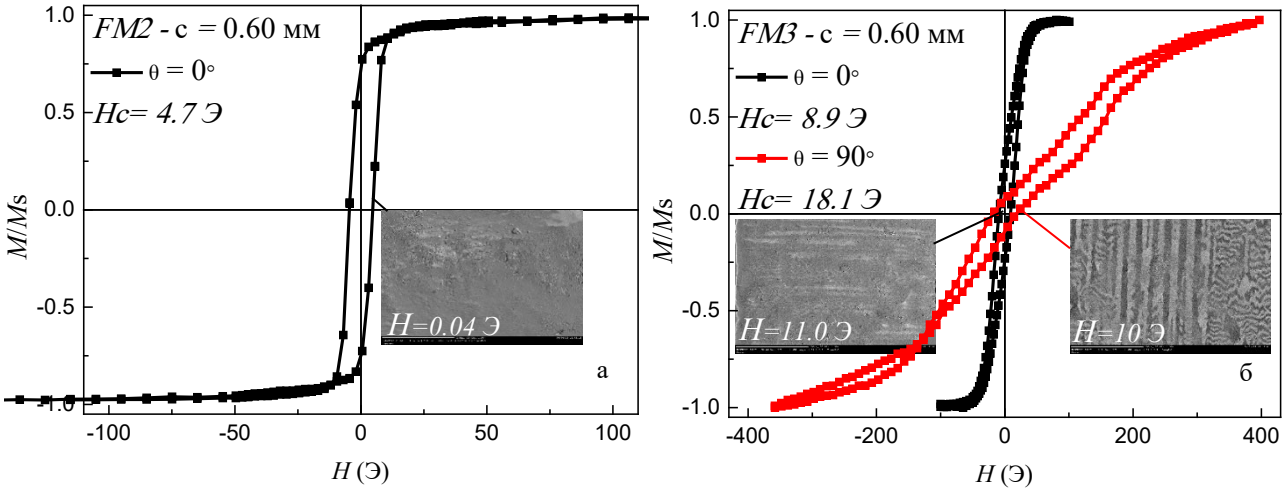
FM2 - c = 0.60 мм
θ = 0°
Hc= 4.7 Э
H=0.04 Э
а
FM3 - c = 0.60 мм
θ = 0°
Hc= 8.9 Э
θ = 90°
Hc= 18.1 Э
H=11.0 Э
H=10 Э
б
M/Ms
H (Э)

Fig. 4.